EDGE ARTICLE

Check for updates

Asymmetrically bridged aroyl-*S,N*-ketene acetal-based multichromophores with aggregation-induced tunable emission†

Lukas Biesen,[a] Julius Krenzer,[a] Nithiya Nirmalananthan-Budau,[b] Ute Resch-Genger [ID] *[b] and Thomas J. J. Müller [ID] *[a]

Asymmetrically bridged aroyl-*S,N*-ketene acetals and aroyl-*S,N*-ketene acetal multichromophores can be readily synthesized in consecutive three-, four-, or five-component syntheses in good to excellent yields by several successive Suzuki-couplings of aroyl-*S,N*-ketene acetals and bis(boronic)acid esters. Different aroyl-*S,N*-ketene acetals as well as linker molecules yield a library of 23 multichromophores with substitution and linker pattern-tunable emission properties. This allows control of different communication pathways between the chromophores and of aggregation-induced emission (AIE) and energy transfer (ET) properties, providing elaborate aggregation-based fluorescence switches.

Introduction

The understanding of the interplay of different, covalently linked nonconjugated chromophores[1,2] is a key step in the evolution of the next generation of functional dyes for photonic applications.[2] A rational fine tuning of the dye building blocks not only enables the combination of the different properties of the constituting chromophores, but the creation of new multi-chromophore systems with advanced features that are more than the sum of their constituents.[3] The communication and intra- and intermolecular interactions of the chromophores play a crucial role for the control of their optical properties and their responsivity to external stimuli.[4] This includes the control of distance- and orientation-dependent energy transfer (ET) like Dexter and Förster processes.[5] To fully exploit the application potential of these multichromophoric systems, their fluorescence properties should be controllable in different aggregation states and environments, ranging from the fluorescence in solution to monomeric or aggregated systems embedded in different matrices and rigidized or aggregated systems in the solid-state.[6] Possible outputs and areas of application are dual emission (aggregation-induced dual emission, AIDE),[7] white light generation,[8] and optical reporters and sensors[9] for bio-analysis,[10] medical diagnostics, and bioimaging.[11] Highly

ambitious concepts for multichromophoric emitters present aggregation-induced emission (AIE)[12] and aggregation-induced enhanced emission (AIEE),[13] which are based on the deactivation of nonradiative pathways by restriction of intramolecular motions (RIM)[14] or by restricted access to conical intersections (RACI).[15] Herein, we present a rational one-pot access to a library of aroyl-*S,N*-ketene acetal based multichromophores[16] in a consecutive diversity-oriented multicomponent synthesis and the tunability of their AIE and ET properties. This qualifies these molecules as aggregation-based fluorescence switches. The highly modular nature of the aroyl-*S,N*-ketene acetals and the simple access to chromophores with different optical properties enables the precise control of the interplay of the different chromophores. Thereby, these multichromophores stand out from other common AIE and ET active systems.[16]
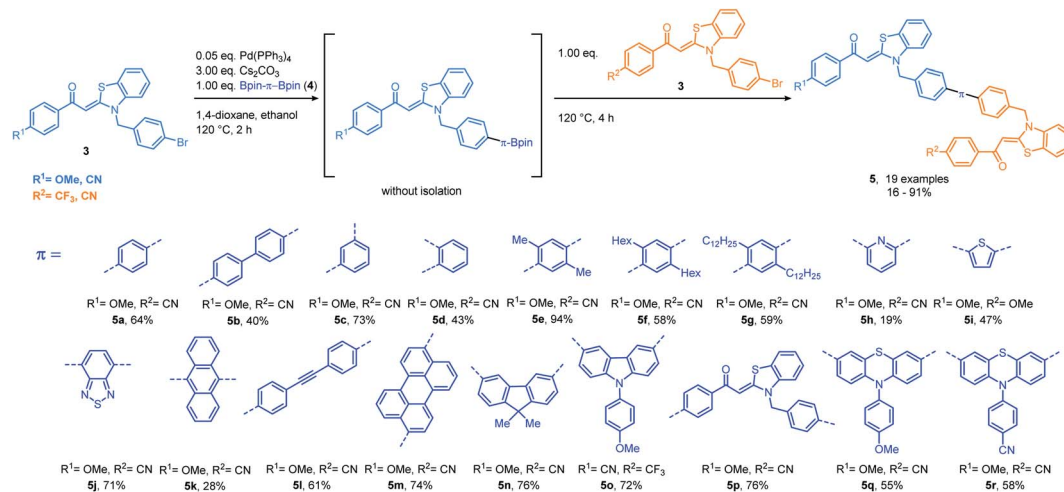
Results and discussion

Synthesis

Previously, we introduced aroyl-*S,N*-ketene acetals as novel AIEgens, where the *N*-benzyl substitution proved essential for the occurrence of AIE.[16] Concatenation of the condensation with a concluding Suzuki coupling gave access to communicating *N*-benzyl aroyl *S,N*-ketene acetal bichromophores with AIE and ET properties.[7b] The multifaceted photophysical and AIE properties of these bichromophores encouraged us to push this concept further by employing different (hetero)aromatic bispinacol esters as linker molecules for developing even more elaborate expanded aroyl *S,N*-ketene acetal multichromophores in a rational one-pot fashion. Starting from electron-donating *p*-bromo substituted benzyl aroyl-*S,N*-ketene acetals, we employ cesium carbonate as a base and bisborylated linker molecules in a Suzuki–Suzuki consecutive three-component reaction in

[a]Institut für Organische Chemie und Makromolekulare Chemie, Heinrich-Heine-Universität Düsseldorf, Universitätsstraße 1, D-40225 Düsseldorf, Germany. E-mail: ThomasJJ.Mueller@uni-duesseldorf.de

[b]Division Biophotonics, Bundesanstalt für Materialforschung und -prüfung (BAM), Department 1, Richard-Willstätter-Straße 11, D-12489 Berlin, Germany

† Electronic supplementary information (ESI) available: Experimental details, characterization, NMR spectra for all new compounds, photophysical data (absorption, emission, aggregation-induced emission), and details of the quantum chemical calculations. See https://doi.org/10.1039/d2sc00415a

Scheme 1 Consecutive three-component Suzuki coupling synthesis of π-bridged aroyl-*S*,*N*-ketene acetal bichromophores 5a–r. All reactions were performed on a 0.50 mmol scale using aroyl-*S*,*N*-ketene acetal 3 (0.50 mmol), bisboronic acid ester 4 (0.50 mmol), Pd(PPh₃)₄ and Cs₂CO₃ (3.0 mmol) in 1,4-dioxane/ethanol 3 : 1 (4.0 mL). The reaction mixtures were stirred at 120 °C for 2 h, then a second aroyl-*S*,*N*-ketene acetal 3 (0.50 mmol) was added and the reaction mixtures were then stirred at 120 °C for 4 h. The yields are given after flash chromatography on silica gel.

a one-pot fashion. Subsequent addition of a second electron-withdrawing *p*-bromo substituted aroyl-*S*,*N*-ketene acetal to the reaction mixture gives access to a library of 19 asymmetric aroyl-*S*,*N*-ketene acetal multichromophores 5 in yields of 16–94% (Scheme 1). By using blue emitting chromophores, we aimed for maximizing the potential of these molecules to undergo ET processes. A plethora of conjugated linker molecules[17] can be implemented in the reaction sequence (for the synthesis of the aroyl-*S*,*N*-ketene acetals and the linker molecules, see ESI (Chapters 3.1–3.4†)). This includes differently substituted benzenes, pyridine, thiophene, benzothiadiazole, anthracene, perylene, bisphenylacetylene, fluorene, carbazole, aroyl-*S*,*N*-ketene acetal and phenothiazines (Scheme 1). Employing consecutive coupling with triborylated benzene and triphenylamine and tetraborylated tetraphenylethene allows to implement three or four different aroyl-*S*,*N*-ketene acetals, thereby selectively generating four enlarged multichromophores 5s–v in moderate yields (48–67%) (Scheme 2). A distinction between the different regioisomers is not possible with this approach. Additionally, a phenanthroline bridged multichromophore is generated in 49% yield by using the established Masuda borylation Suzuki arylation sequence[18] (for further details, see ESI Scheme S1†). Subsequently, the absorption and emission properties of the novel multichromophoric dyes 5 are thoroughly studied in the solid state, in solvent mixtures of different polarity, and incorporated into polystyrene microparticles.

Absorption and emission studies in the solid-state

All aroyl-*S*,*N*-ketene acetal-based chromophore systems investigated so far enabled a tuning of their solid-state rainbow-colored emission by variation of the electronic nature of the substituents in *para*-position of the aroyl moiety.[16] The novel aroyl-*S*,*N*-ketene acetal multichromophores are no exception to this rule. In contrast to previous systems, substituents in *para*-
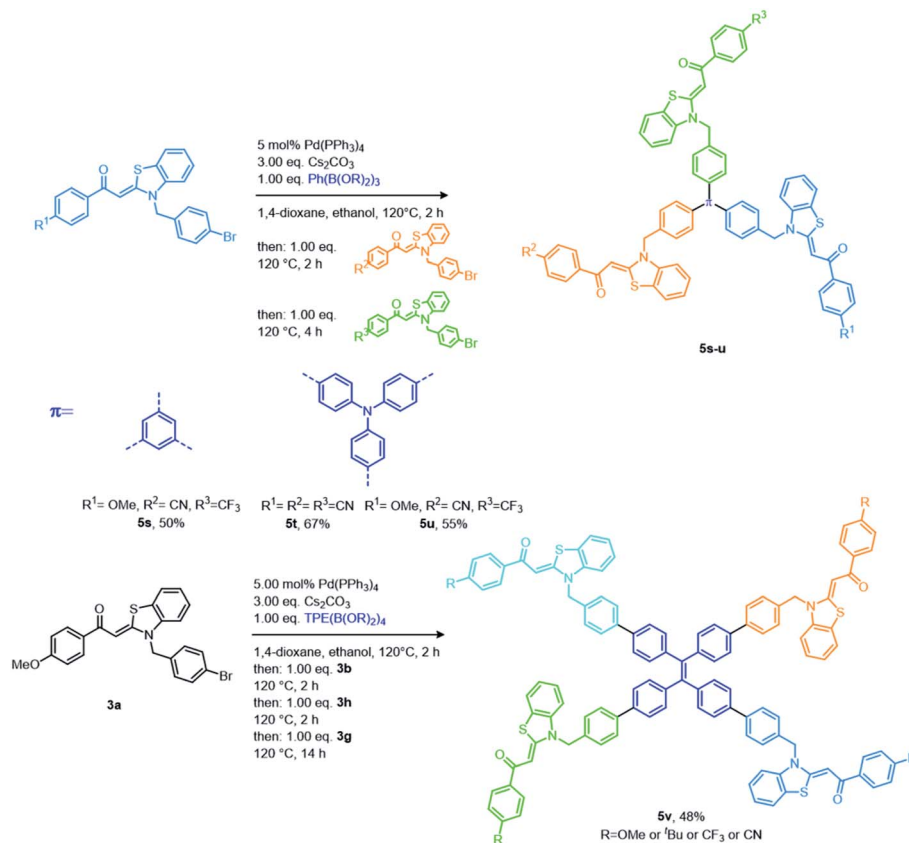
position of the aroyl moiety were now kept constant and only the linker molecules were changed. Consequently, color tuning is still feasible, but the covered emission color range is narrowed. Nevertheless, the multichromophoric dyes 5 can be readily distinguished by their solid-state emission color ranging from greenish to orange-red (Fig. 1). Thiophene bridged multichromophore 5i exhibits the shortest wavelength emission maximum (λ_{em} = 524 nm), while the benzothiadiazole bridged multichromophore 5j displays the most red-shifted emission maximum (λ_{em} = 566 nm) (Fig. 1; for details see ESI, Chapters 7 and 8†). Subsequently done measurements of the solid-state fluorescence quantum yields (Φ_f) of selected multichromophores 5 revealed only low Φ_f values of 0.01 to 0.04 for most of multichromophores 5. However, the phenylene and xylene bridged dyes 5a and 5e have increased Φ_f of 0.10 and 0.11, respectively, presumably due to the proximity of both solid-state emissive aroyl-*S*,*N*-ketene acetals. Also the aroyl-*S*,*N*-ketene acetal bridged multichromophore 5p has a slightly higher Φ_f of 0.08. The highest Φ_f of 0.16 was observed for star-shaped multichromophore 5s.

Absorption and fluorescence in ethanol

The absorption maxima of the aroyl-*S*,*N*-ketene acetal multichromophore family 5 vary between 250 and 400 nm. Our previous studies suggest that the absorption maxima around 400 nm can be ascribed to the aroyl-*S*,*N*-ketene acetal core,[3] while maxima occurring in the wavelength region of 250 nm to 330 nm can be unequivocally ascribed to the different linker molecules. Apparently, the multichromophores' absorption maxima originate from the sum of the absorption bands of the constituents of each dye.

With exception of the dimethylamino-substituted aroyl-*S*,*N*-ketene acetal,[16] aroyl-*S*,*N*-ketene acetals do not fluoresce in solution. Thus, the observed luminescence of our multichromophores is ascribed to the linker molecules. Except for

Scheme 2 Consecutive four-component and five-component Suzuki coupling synthesis of aroyl-*S,N*-ketene acetal multichromophores **5s–v**. All reactions were performed on a 0.50 mmol scale: aroyl-*S,N*-ketene acetal **3** (0.50 mmol), bisboronic acid ester **4** (0.50 mmol), Pd(PPh$_3$)$_4$ and Cs$_2$CO$_3$ (3.0 mmol) in 1,4-dioxane/ethanol 3 : 1 (4.0 mL) were stirred at 120 °C for 2 h, then additional aroyl-*S,N*-ketene acetals **3** (0.50 mmol) were added stepwise and the reaction mixture stirred at 120 °C for 2 h. After addition of the final aroyl-*S,N*-ketene acetals **3**, the reaction mixture was stirred at 120 °C for 4 h. The yields given in % present the yields obtained after flash chromatography on silica gel.

the phenylene and bisphenylene bridged dyes **5a** and **5b** and the tetraphenylethene bridged multichromophore **5v**, all multichromophores emit mostly blue light in solution (λ_{em} = 440–470 nm). Only benzothiadiazole and perylene bridged dyes **5j** and **5m** show a green fluorescence in the wavelength region of λ_{em} of 479–500 nm (for details, see ESI, Table S9 and Chapter 7†). Φ_f of dyes **5** in ethanol have values in the range between of 0.01 to 0.05. Moreover, solely anisylcarbazole aroyl-*S,N*-ketene acetal **5o** exhibits an excitation wavelength dependence of its emission. For this dye, excitation at 395 nm leads to a weak emission maximum at 500 nm, whereas excitation at 295 nm, where also the short wavelength emissive phenylcarbazol moiety is excited, two emission maxima can be observed, one at 500 nm and one at 380 nm.[19] This is ascribed to the simultaneous emission of both chromophores at this excitation wavelength. Therefore, we assume that a partial ET is operative in carbazole linked multichromophore **5o**, similarly as observed for the phenylcarbazole bichromophore in our previous work.[7b]

AIE studies

Aggregation-induced emission (AIE) and aggregation-induced enhanced emission (AIEE) have proved to be characteristic for aroyl-*S,N*-ketene acetal-based chromophores. Therefore, and

encouraged by the observed solid-state emission, we performed AIE studies with multichromophores **5**. Most of the multichromophores **5** are soluble in common, polar organic solvents such as acetonitrile, THF, 1,4-dioxane, and ethanol, but insoluble in water. Multichromophore **5s–v** with their enlarged π-electron systems are more hydrophobic and have a reduced solubility in these solvents. Therefore, for these dyes lower concentrations had to be used. Subsequently, samples of the bichromophores were diluted in different organic solvent/water mixtures with water contents varying from 0% to 95%. As previously observed for aroyl-*S,N*-ketene acetals, the most promising spectroscopic results were obtained in ethanol/water mixtures, which were therefore used for all further AIE studies. These data are representatively discussed in detail for selected examples of each class of bichromophores. Due to solubility reasons, multichromophore **5u** was examined in acetone/water mixtures.

As shown in Fig. 2, upon aggregation, dyes **5e**, **5f**, and **5g** exhibit a similar fluorescence behavior in terms of emission color and band shape. At a low water fraction, the chromophores only fluoresce very weakly (Φ_f < 0.01). With an increase of the water content, the compounds begin to aggregate, thus resulting in a bathochromic shift of the emission maxima from
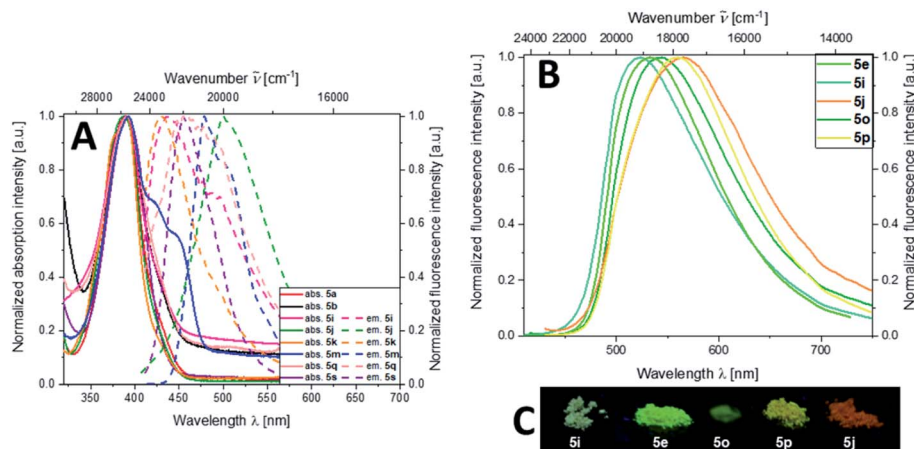
Fig. 1 (A) Normalized absorption and emission spectra of selected bridged aroyl-*S,N*-ketene acetals **5** in ethanol using dye concentrations of 10^{-5} M (absorption) and 10^{-7} M (emission; $\lambda_{exc} = \lambda_{abs,max}$); (B) normalized solid-state emission spectra; (C, right) solid-state fluorescence colors of selected bridged aroyl-*S,N*-ketene acetals **5** ($\lambda_{exc} = 365$ nm) revealing the rainbow-colored fluorescence and emission color tuning by substitution pattern. The absorption and fluorescence measurements were done at $T = 298$ K with a calibrated photometer and a calibrated fluorometer; the fluorescence was excited at the absorption maximum ($\lambda_{exc} = \lambda_{abs,max}$).
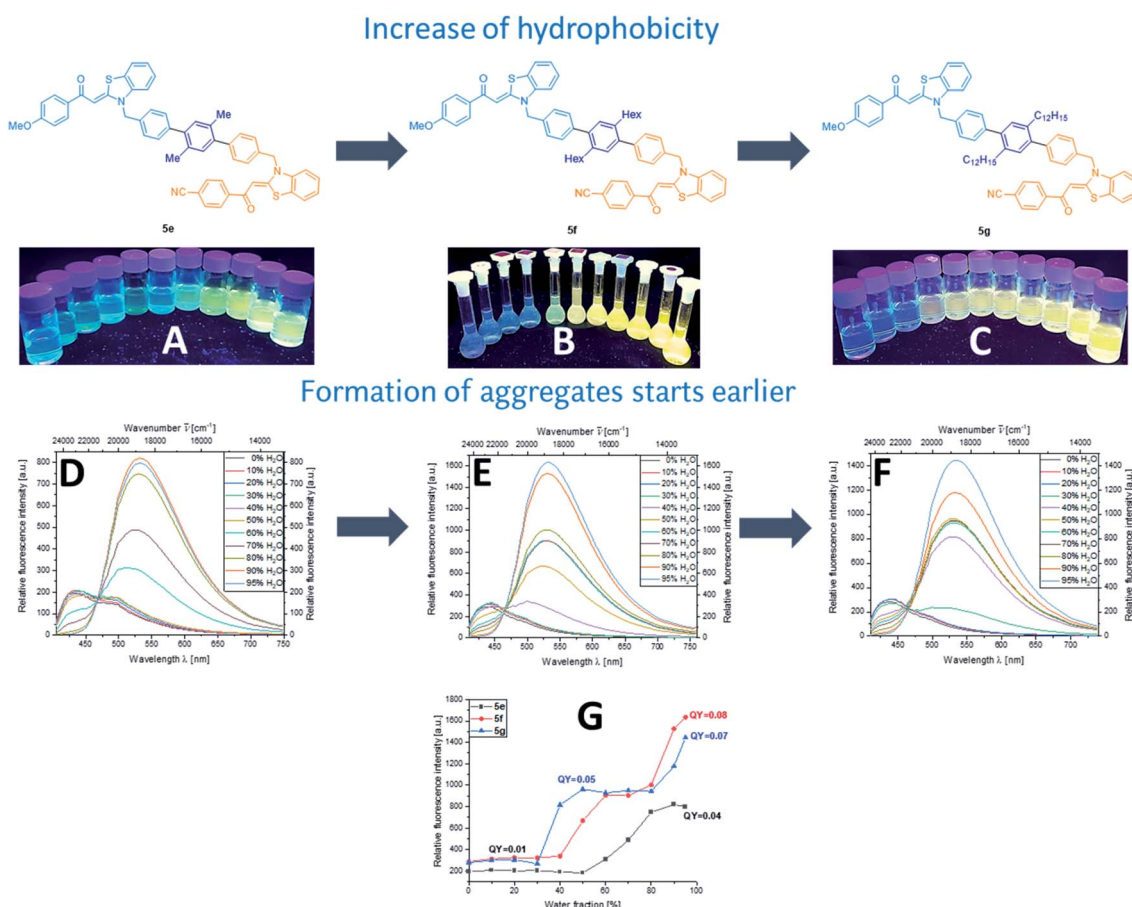

Fig. 2 (Top, from left to right) Visualization (photographs) of the AIE features of **5e** (A), **f** (B) and **g** (C) in ethanol/water mixtures of increasing water content upon excitation with a UV-lamp ($c = 10^{-7}$ M, $\lambda_{exc} = 365$ nm); (Middle) emission spectra of **5e** (D), **f** (E) and **g** (F) in ethanol/water upon increasing water content revealing an earlier start of aggregation (recorded at $T = 298$ K, $c = 10^{-7}$ M, λ_{exc} (**5e**) = 385 nm, λ_{exc} (**5f**) = 390 nm, and λ_{exc} (**5f**) = 390 nm); (G) comparison of fluorescence intensity of compounds **5e**, **f** and **g** upon aggregation.

around 450 to 550 nm and in enhanced Φ_f values of 0.07–0.08. This equals an increase in fluorescence by factors of 4 to 5. These effects are ascribed to a blocking of non-radiative decay of the excited singlet state by RIM[14] or to a restricted access to conical intersections (RACI).[15]

Interestingly, our results also underline the control of the onset of dye aggregation by varying the aliphatic chain length attached to the phenylene linker and thereby, dye hydrophobicity. Whereas xylene bridged dye **5e** starts to aggregate at a water fraction of 60%, prolonging the linker, shifts the onset of aggregation to a lesser water content, *e.g.* to a water content of 40% for a hexyl chain. Incorporating two dodecyl substituents into the phenylene linker, yielding more hydrophobic **5g**, leads to aggregation already at a water fraction of 30% (Fig. 2). Furthermore, an increasing aliphatic chain length also results in an enhanced steric hindrance thereby reducing π–π-stacking. This can further elevate AIE effects.

The most remarkable AIE behavior was observed for anisylcarbazole bridged chromophore **5o** and triphenylamine star shaped multichromophore **5u**, both revealing an excitation wavelength dependent fluorescence. Excitation at $\lambda_{exc} = 295$ nm leads to the blue emission of the anisylcarbazole chromophore. Consequently, at low water fractions, only the emission band of the carbazole is observed. At water fractions above 40%, a second band appears at 525 nm, that originates from the aroyl-*S,N*-ketene acetal unit. Simultaneously, the carbazole emission is diminished and finally completely quenched. Upon excitation at the longest wavelength maximum of 395 nm only the emission band of the aroyl-*S,N*-ketene acetal is observed. These findings are further underpinned by measurements of Φ_f and the fluorescence lifetime τ. For $\lambda_{exc} = 395$ nm, Φ_f amounts to 0.02 and τ is below 1 ns. Upon excitation at 252 nm, Φ_f increases to 0.06 but is eventually reduced upon further aggregation. This goes hand in hand with the disappearance of the carbazole emission band. This effect is even more pronounced

in time-resolved fluorescence studies. With a τ of 6–8 ns at lower water fractions, **5o** displays a remarkably long lifetime. The maximum value of τ is reached at the onset of the appearance of dual emission. Again, in parallel with the disappearance of the carbazole emission band, τ is reduced. Therefore, we conclude that the observed mixed emission color originates from a rare dual emission, which is a clear hint for an emerging energy transfer (Fig. 3, right). This dual fluorescence is possibly caused by the AIE characteristics of both chromophores in combination with solvent-induced changes of the spectral position of the absorption and emission bands and hence the spectral overlap of the emission of the anisylcarbazole donor and the aroyl-*S,N*-ketene acetal acceptor. This can have a significant effect on the ET efficiency. In the aggregates, a partial (frustrated) intra- and intermolecular energy transfer[4–6,20] can occur from the anisylcarbazole donor to the aroyl-*S,N*-ketene acetal acceptor yielding an aggregation-induced dual emission (AIDE).

Triphenylamine multichromophore **5u** reveals a similar behavior. Exciting the triphenylamine chromophore at 330 nm yields an emission band at 420 nm. This fluorescence disappears at a higher water fraction while simultaneously a second emission band appears at 540 nm, which is ascribed to the aroyl-*S,N*-ketene acetal. This intertwining aggregation behavior of emission-quenched triphenylamine and emission-enhanced aroyl-*S,N*-ketene acetal give rise to AIDE. Selective excitation of the aroyl-*S,N*-ketene acetal unit at 387 nm results in a different behavior, *i.e.*, the observation of only the emission band of the aroyl-*S,N*-ketene acetal acceptor. Again, the Φ_f maximum is reached at water fractions of 50–70% where intertwining aggregation and potential energy transfer are effective. The same trend can be observed for τ which is more than five times higher when the dual emission starts to appear (Fig. 3, right).

Overall, the presented photophysical data clearly illustrate the possibility to simultaneously exploit the photophysical properties of linker molecules and aroyl-*S,N*-ketene acetals. Therefore, the
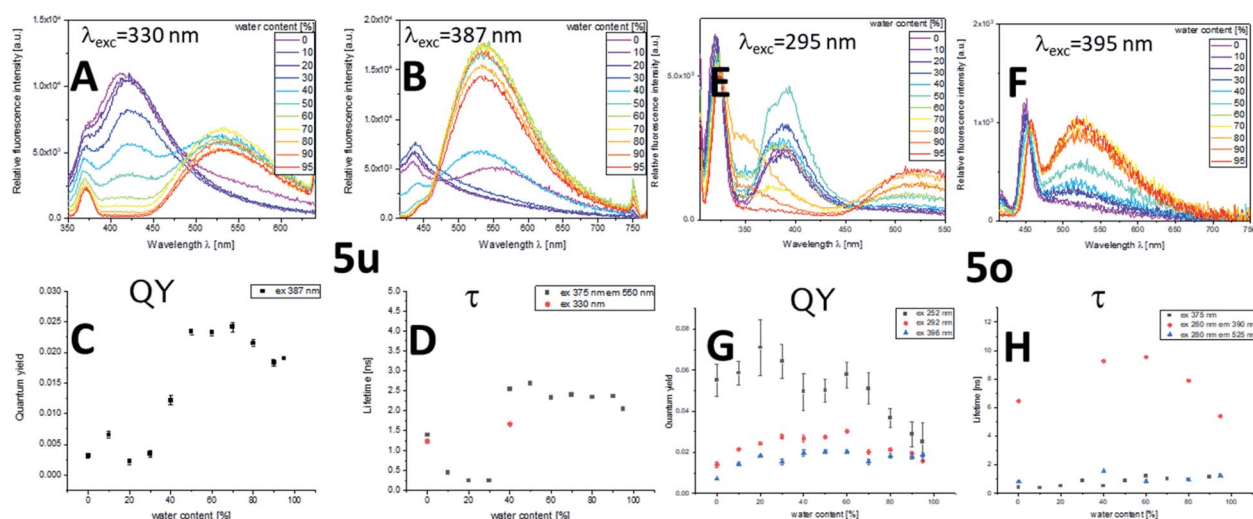

Fig. 3 (Top, left) Emission spectra of **5o** in acetone/water mixtures upon increasing water content (λ_{exc} (**5o**) = 295 nm (A), λ_{exc} (**5o**) = 395 nm (B)); (Top, right) emission spectra of **5u** in acetone/water mixtures upon increasing water content (λ_{exc} (**5u**) = 330 nm (E), λ_{exc} (**5u**) = 387 nm (F)); (Bottom, left) Φ_f (C) and τ (D) of **5o** depending on the water fraction of the acetone/water mixture; (Bottom, right) Φ_f (G) and τ (H) of **5u** depending on the water fraction of the acetone/water mixture. The measurements were done at $T = 298$ K using dye concentrations of 10^{-7} M.
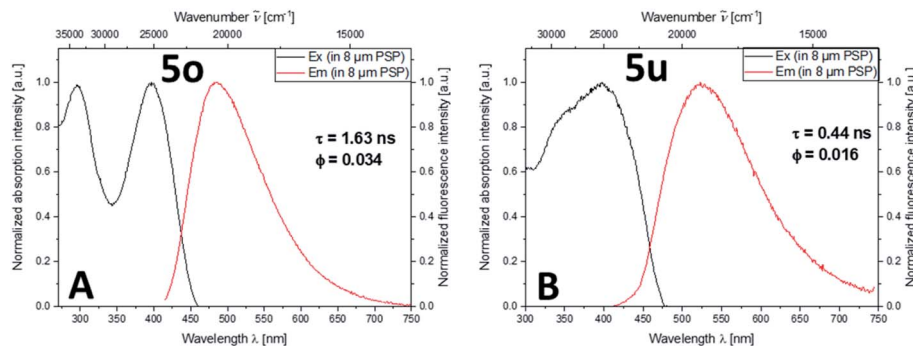
Fig. 4 Normalized fluorescence excitation and emission spectra (λ_{exc} = 401 nm) of 8 μm-sized PSP loaded with dye **5o** (A) and dye **5u** (B) dispersed in water.

photophysical features of these multichromophores are more favorable than the properties of the individual moieties constituting these molecules. The linker molecules control the fluorescence in solution while the solid-state emission properties and the AIE behavior can be fine-tuned by the interplay of linker and aroyl-S,N-ketene acetals that is responsible for the ET efficiency and the nature of aggregation. Enlarged flat π-systems as linker molecules lead to a drastically reduced AIE behavior, whereas sterically demanding and nonpolar linkers encourage a more pronounced AIE behavior. Furthermore, the emission color and intensity of multichromophores **5** can be established by combining the respective aroyl-S,N-ketene acetals and linker molecules in a rational tool box approach (for details, see ESI Chapter 8†) for applications as polarity sensors and in analytics as previously shown.[7b,16]

Encapsulation of selected multichromophores in polystyrene particles

Encapsulating aroyl-S,N-ketene acetals in a nonpolar solid matrix like polystyrene can improve the fluorescence properties of the multichromophores **5**. Particularly, it can enhance Φ_f and τ by sterically restricting or attenuating intramolecular rotations of the matrix-entrapped dye molecules.[21] For these studies, exemplarily, phenylcarbazole bridged multichromophore **5o** and triphenylamine multichromophore **5u** were chosen due to their intense solid-state fluorescence and pronounced AIE behavior. A high encapsulation concentration (6 mM) was used to ensure an enhanced probability of dye–dye interactions in the 8 μm polystyrene particles (PSP). The emission spectra of PSP stained with **5o** and **5u** (Fig. 4) reveal an emission behavior similar to the AIE behavior of these chromophores in ethanol–water mixtures when excited at the longest absorption maximum. Due to the dual emission observed in the aggregated state, excitation at 295 nm was applied as well. However, in contrast to previous AIE studies this did not lead to a different emission behavior, indicating the absence of ET processes. Additionally, upon PSP encapsulation Φ_f is increased to 0.034 (**5o**) and 0.016 (**5u**), surpassing Φ_f found for **5o** and **5u** in ethanol, ethanol–water mixtures, and in the solid-state. Simultaneously, τ increased to 1.63 ns (**5o**) and 0.44 ns (**5u**).

Conclusion and outlook

In summary, a highly diverse library of 23 bridged aroyl-S,N-ketene acetals and aroyl-S,N-ketene acetal-based multichromophores was generated with moderate to excellent yields in a one-pot fashion by either three-, four-, or five-component Suzuki reactions. The emission behavior of all chromophores was thoroughly studied in the solid-state, in organic solvents, upon aggregation induced in mixtures of organic solvents and water and encapsulated in polystyrene particles (PSP). These spectroscopic studies confirm the substitution pattern control of the solid-state emission color and the aggregation-induced emission (AIE) of the dyes. The nature of the linker molecule determines the underlying different communication pathway for all chromophores and the aggregation behavior, *i.e.*, the onset of aggregation in mixtures of organic solvents and water. The latter is ascribed to the tuning of the dye hydrophobicity by the length and chemical nature of the linker. Complete or partial energy transfer, modulated by the linker molecule, was observed for selected multichromophores **5o** and **5u**, leading to a dual emission or an aggregation-induced switching of the fluorescence.

As demonstrated in this study, the interplay of different chromophores and linker molecules is the key to the rational design of multichromophoric emitters and the control of (partial) energy transfer in aggregates and in solution. In the future, we will perform detailed mechanistic studies to confirm the control of the photophysical properties of aroyl-S,N-ketene acetals required for exploiting and fine-tuning the application potential of this dye class.

Data availability

The datasets supporting this article have been uploaded as part of the ESI.†

Author contributions

T. J. J. M. and U. R.-G. conceived the idea. L. B. synthesized all the compounds and identified AIE properties. J. K. synthesized four components. N. N.-B. conducted and discussed the

photophysical experiments and AIE characteristics. L. B. wrote the manuscript's first draft, and all authors discussed and commented on the manuscript. T. J. J. M. directed the project.

Conflicts of interest

There are no conflicts to declare.

Acknowledgements

Notes and references

1 (a) A. Lapini, P. Fabbrizzi, M. Piccardo, M. di Donato, L. Lascialfari, P. Foggi, S. Cicchi, M. Biczysko, I. Carnimeo and F. Santoro, *Phys. Chem. Chem. Phys.*, 2014, **16**, 10059; (b) S. A. Sharber, K.-C. Shih, A. Mann, F. Frausto, T. E. Haas, M.-P. Nieh and S. W. Thomas, *Chem. Sci.*, 2018, **9**, 5415–5426; (c) A. S. Klymchenko, D. A. Yushchenko and Y. Mély, *J. Photochem. Photobiol., A*, 2007, **192**, 93; (d) R. Gómez, J. L. Segura and N. Martin, *Chem. Commun.*, 1999, 619–620.

2 (a) E. De Meulenaere, W.-Q. Chen, S. Van Cleuvenbergen, M.-L. Zheng, S. Psilodimitrakopoulos, R. Paesen, J.-M. Taymans, M. Ameloot, J. Vanderleyden, P. Loza-Alvarez, X.-M. Duan and K. Clays, *Chem. Sci.*, 2012, **3**, 984–995; (b) B. Saha, B. Ruidas, S. Mete, C. Das Mukhopadhyay, K. Bauri and P. De, *Chem. Sci.*, 2020, **11**, 141–147; (c) M. Murai, S.-Y. Ku, N. D. Treat, M. J. Robb, M. L. Chabinyc and C. J. Hawker, *Chem. Sci.*, 2014, **5**, 3753–3760; (d) S. Cekli, R. W. Winkel, E. Alarousu, O. F. Mohammed and K. S. Schanze, *Chem. Sci.*, 2016, **7**, 3621–3631.

3 (a) S. Guo, J. Zhao, B. Küçüköz, A. Karatay, M. Hayvali, H. G. Yaglioglu and A. Elmali, *Chem. Sci.*, 2014, **5**, 489–500; (b) Z. Guo, W. Zhu and H. Tian, *Chem. Commun.*, 2012, **48**, 6073–6084.

4 (a) G. C. Bazan, *J. Org. Chem.*, 2007, **72**, 8615; (b) E. Collini, *Phys. Chem. Chem. Phys.*, 2012, **14**, 3725–3736.

5 (a) Q. Y. Yang and J. M. Lehn, *Angew. Chem., Int. Ed.*, 2014, **53**, 4572; (b) L. Yuan, W. Lin, K. Zheng and S. Zhu, *Acc. Chem. Res.*, 2013, **46**, 1462–1473; (c) Z. Zhang, Y.-S. Wu, K.-C. Tang, C.-L. Chen, J.-W. Ho, J. Su, H. Tian and P.-T. Chou, *J. Am. Chem. Soc.*, 2015, **137**, 8509; (d) B. Xu, Y. Mu, Z. Mao, Z. Xie, H. Wu, Y. Zhang, C. Jin, Z. Chi, S. Liu and J. Xu, *Chem. Sci.*, 2016, **7**, 2201.

6 (a) L. Xu, W. Lin, B. Huang, J. Zhang, X. Long, W. Zhang and Q. Zhang, *J. Mater. Chem. C*, 2021, **9**, 1520–1536; (b) J. Zhou, L. Stojanovic, A. A. Berezin, T. Battisti, A. Gill, B. M. Kariuki, D. Bonifazi, R. Crespo-Otero, M. R. Wasielewski and Y.-L. Wu, *Chem. Sci.*, 2021, **12**, 767–773.

7 (a) M. Denißen, R. Hannen, D. Itskalov, L. Biesen, N. Nirmalananthan-Budau, K. Hoffmann, G. J. Reiss, U. Resch-Genger and T. J. J. Müller, *Chem. Commun.*, 2020, **56**, 7407; (b) L. Biesen, L. May, N. Nirmalananthan-Budau, K. Hoffmann, U. Resch-Genger and T. J. J. Müller, *Chem.–Eur. J.*, 2021, **27**, 13426–13434; (c) Z. He, W. Zhao, J. W. Lam, Q. Peng, H. Ma, G. Liang, Z. Shuai and B. Z. Tang, *Nat. Commun.*, 2017, **8**, 1; (d) X. Feng, C. Qi, H.-T. Feng, Z. Zhao, H. H. Y. Sung, I. D. Williams, R. T. K. Kwok, J. W. Y. Lam, A. Qin and B. Z. Tang, *Chem. Sci.*, 2018, **9**, 5679–5687.

8 (a) M. Börgardts and T. J. J. Müller, *Beilstein J. Org. Chem.*, 2017, **13**, 768; (b) G. Zhang, H. Bala, Y. Cheng, D. Shi, X. Lv, Q. Yu and P. Wang, *Chem. Commun.*, 2009, 2198–2200; (c) M. Tominaga, H. Naito, Y. Morisaki and Y. Chujo, *New J. Chem.*, 2014, **38**, 5686; (d) P. P. Neelakandan, A. Jiménez and J. R. Nitschke, *Chem. Sci.*, 2014, **5**, 908–915.

9 (a) B. Xu, Y. Mu, Z. Mao, Z. Xie, H. Wu, Y. Zhang, C. Jin, Z. Chi, S. Liu, J. Xu, Y.-C. Wu, P.-Y. Lu, A. Lien and M. R. Bryce, *Chem. Sci.*, 2016, **7**, 2201–2206; (b) S. Sinha, B. Chowdhury, U. K. Ghorai and P. Ghosh, *Chem. Commun.*, 2019, **55**, 5127–5130; (c) N. I. Georgiev, A. I. Said, R. A. Toshkova, R. D. Tzoneva and V. B. Bojinov, *Dyes Pigm.*, 2019, **160**, 28; (d) X. Li, G. Baryshnikov, C. Deng, X. Bao, B. Wu, Y. Zhou, H. Ågren and L. Zhu, *Nat. Commun.*, 2019, **10**, 1.

10 (a) Y. Gabe, T. Ueno, Y. Urano, H. Kojima and T. Nagano, *Anal. Bioanal. Chem.*, 2006, **386**, 621–626; (b) A. S. Klymchenko, *Acc. Chem. Res.*, 2017, **50**, 366.

11 (a) G. Zhang, G. M. Palmer, M. W. Dewhirst and C. L. Fraser, *Nat. Mater.*, 2009, **8**, 747; (b) Y. S. Marfin, A. V. Solomonov, A. S. Timin and E. V. Rumyantsev, *Curr. Med. Chem.*, 2017, **24**, 2745–2772.

12 (a) J. Mei, N. L. Leung, R. T. Kwok, J. W. Lam and B. Z. Tang, *Chem. Rev.*, 2015, **115**, 11718; (b) J. Mei, Y. Hong, J. W. Lam, A. Qin, Y. Tang and B. Z. Tang, *Adv. Mater.*, 2014, **26**, 5429; (c) Z. He, C. Ke and B. Z. Tang, *ACS Omega*, 2018, **3**, 3267–3277; (d) Z. Zhao, H. Zhang, J. W. Y. Lam and B. Z. Tang, *Angew. Chem., Int. Ed.*, 2020, **59**, 9888–9907.

13 (a) B.-K. An, S.-K. Kwon, S.-D. Jung and S. Y. Park, *J. Am. Chem. Soc.*, 2002, **124**, 14410; (b) F. Würthner, *Angew. Chem., Int. Ed.*, 2020, **59**, 14192; (c) N. L. C. Leung, N. Xie, W. Yuan, Y. Liu, Q. Wu, Q. Peng, Q. Miao, J. W. Y. Lam and B. Z. Tang, *Chem.–Eur. J.*, 2014, **20**, 15349–15353.

14 (a) Y. Tu, Z. Zhao, J. W. Y. Lam and B. Z. Tang, *Natl. Sci. Rev.*, 2021, **8**, 1–4; (b) J. Zhang, H. Zhang, J. W. Y. Lam and B. Z. Tang, *Chem. Res. Chin. Univ.*, 2021, **37**, 1–15.

15 (a) X.-L. Peng, S. Ruiz-Barragan, Z.-S. Li, Q.-S. Li and L. Blancafort, *J. Mater. Chem. C*, 2016, **4**, 2802–2810; (b) Y. Tu, J. Liu, H. Zhang, Q. Peng, J. W. Y. Lam and B. Z. Tang, *Angew. Chem., Int. Ed.*, 2019, **131**, 15053–15056.

16 L. Biesen, N. Nirmalananthan-Budau, K. Hoffmann, U. Resch-Genger and T. J. J. Müller, *Angew. Chem., Int. Ed.*, 2020, **59**, 10037.

17 (*a*) L. Mayer, L. May and T. J. J. Müller, *Org. Chem. Front.*, 2020, **7**, 1206–1217; (*b*) M. Paramasivam, A. Gupta, N. J. Babu, K. Bhanuprakash, S. V. Bhosale and V. J. Rao, *RSC Adv.*, 2016, **6**, 66978–66989; (*c*) S.-L. Deng, T.-L. Chen, W.-L. Chien and J.-L. Hong, *J. Mater. Chem. C*, 2014, **2**, 651–659; (*d*) F. S. Han, M. Higuchi and D. G. Kurth, *Org. Lett.*, 2007, **9**, 559–562; (*e*) S. F. Völker, M. Renz, M. Kaupp and C. Lambert, *Chem.–Eur. J.*, 2011, **17**, 14147–14163; (*f*) S. Dalapatim, E. Jin, M. Addicoat, T. Heine and D. Jiang, *J. Am. Chem. Soc.*, 2016, **138**, 5797–5800.

18 (*a*) E. Merkul, E. Schäfer and T. J. J. Müller, *Org. Biomol. Chem.*, 2011, **9**, 3139–3141; (*b*) N. Rehberg, G. A. Sommer, D. Drießen, M. Kruppa, E. T. Adeniyi, S. Chen, L. Wang, K. Wolf, B. O. A. Tasch, T. R. Ioerger, K. Zhu, T. J. J. Müller and T. Kalscheuer, *J. Med. Chem.*, 2020, **63**, 12623–12641; (*c*) L. Biesen and T. J. J. Müller, *Aggregate*, 2021, **2**, e105.

19 J. Yuan, L. Jin, R. Chen, X. Tang, X. Xie, Y. Tang and W. Huang, *New J. Chem.*, 2018, **42**, 14704–14708.

20 (*a*) S. Park, J. E. Kwon, S. H. Kim, J. Seo, K. Chung, S.-Y. Park, D.-J. Jang, B. M. Medina, J. Gierschner and S. Y. Park, *J. Am. Chem. Soc.*, 2009, **131**, 14043–14049; (*b*) Y. Lei, Q. Liao, H. Fu and J. Yao, *J. Am. Chem. Soc.*, 2010, **132**, 1742–1743.

21 (*a*) T. Behnke, C. Würth, K. Hoffmann, M. Hübner, U. Panne and U. Resch-Genger, *J. Fluoresc.*, 2011, **21**, 937–944; (*b*) T. Behnke, C. Würth, E.-M. Laux, K. Hoffmann and U. Resch-Genger, *Dyes Pigm.*, 2012, **94**, 247–257.